Article

SOURCE DATA | TRANSPARENT PROCESS

EMBO reports

# Serum amyloid A promotes LPS clearance and suppresses LPS-induced inflammation and tissue injury

Ni Cheng[1], Yurong Liang[1], Xiaoping Du[1] & Richard D Ye[1,2,*]

## Abstract

**Lipopolysaccharide (LPS) is a major microbial mediator for tissue injury and sepsis resulting from Gram-negative bacterial infection. LPS is an external factor that induces robust expression of serum amyloid A (SAA), a major constituent of the acute-phase proteins, but the relationship between SAA expression and LPS-induced tissue injury remains unclear. Here, we report that mice with inducible transgenic expression of human SAA1 are partially protected against inflammatory response and lung injury caused by LPS and cecal ligation and puncture (CLP). In comparison, transgenic SAA1 does not attenuate TNFα-induced lung inflammation and injury. The SAA1 expression level correlates inversely with the endotoxin concentrations in serum and lung tissues since SAA1 binds directly to LPS to form a complex that promotes LPS uptake by macrophages. Disruption of the SAA1-LPS interaction with a SAA1-derived peptide partially reduces the protective effect and exacerbates inflammation. These findings demonstrate that acute-phase SAA provides innate feedback protection against LPS-induced inflammation and tissue injury.**

**Keywords** acute-phase response; inflammation; innate immunity; lipopolysaccharide; serum amyloid A

**Subject Categories** Immunology; Microbiology, Virology & Host Pathogen Interaction

**DOI** 10.15252/embr.201745517 | Received 19 November 2017 | Revised 24 July 2018 | Accepted 27 July 2018 | Published online 20 August 2018

**EMBO Reports (2018) 19: e45517**

## Introduction

Host response to microbial infection utilizes a multitude of innate and specific mechanisms that collectively constitute antimicrobial immunity. Whereas T and B lymphocytes are primary cells for adaptive immunity with their characteristic memory and specificity, innate immune cells such as macrophages and neutrophils recognize pathogen-associated molecular patterns using pattern recognition receptors such as the Toll-like receptors. Innate immunity is found not only in mammals but also in lower species such as *Drosophila* [1]. One of the conserved host responses to infection, trauma, and environmental stress is the acute-phase response [2], which is a systemic reaction characterized with enhanced expression of a set of acute-phase proteins [3]. Induced expression of major acute-phase proteins such as serum amyloid A (SAA) and C-reactive proteins (CRP) is robust, with serum concentrations of these proteins rising as high as 1,000-fold [4]. Studies have shown that elevated expression of SAA and CRP is characteristic of all inflammatory diseases [3]. In addition, SAA expression is highly induced following surgery and severe tissue injury, and in late-stage malignancy [5]. Despite wide acceptance of SAA and CRP as major biomarkers of inflammatory diseases and malignance, the biological functions of these proteins remain poorly understood [6,7].

SAA refers to a family of proteins encoded by several different genes. In humans, the SAA proteins are encoded by two inducible genes, SAA1 and SAA2, and a constitutively expressed gene, SAA4. In mice, an additional gene, SAA3, encodes an inducible form of SAA with high structural similarities to other SAA proteins [8]. Acute-phase human SAA, referring to the inducible forms of SAA, are proteins of 103–104 amino acids consists of four alpha-helices that bundle together to form hexamers [9]. A variety of cells, including hepatocytes, macrophages, and colon epithelial cells, produce SAA proteins upon stimulation with infectious and inflammatory factors such as LPS, IL-1β, and IL-6 [4]. Secreted SAA proteins function in a paracrine manner in inflammatory tissues [10] and bind to high-density lipoprotein (HDL) in the plasma [11]. In addition to these properties, SAA is a precursor of amyloid A that deposits to major organs and causes secondary amyloidosis [2,12].

The biological functions of SAA in host defense and immunity are ambiguously defined. SAA has been shown to be chemotactic to phagocytes and T lymphocytes [13], although its structure is completely different from chemokines and classic chemoattractants such as C5a [9]. *In vitro* studies have shown that SAA stimulates a variety of leukocytes to secrete cytokines including IL-1β, IL-6, and TNFα [14], but unlike these inflammatory factors, SAA is not generally considered a cytokine [10]. Recent identification of acute-phase SAA as a mediator of local effector Th17 response driven by gut microbiome [15,16] has prompted a careful examination of SAA for its

1 Department of Pharmacology and Center for Lung and Vascular Biology, College of Medicine, University of Illinois, Chicago, IL, USA
2 State Key Laboratory for Quality Research in Chinese Medicine, Institute of Chinese Medical Sciences, University of Macau, Macau Special Administrative Region, China
*Corresponding author. Tel: +853 88224690; E-mail: richardye@umac.mo

cytokine-like activities, tissue expression profile, signaling properties, and *in vivo* functions in host defense and inflammation. It is notable that the majority of the published reports on the proinflammatory activities of SAA were generated using recombinant human SAA that is a hybrid of the SAA1 and SAA2 isoforms expressed in *Escherichia coli* [17]. Therefore, the *in vivo* functions of SAA in inflammatory diseases remain to be investigated. To this end, we prepared transgenic mice that express human SAA1 under the direction of the scavenger receptor A promoter–enhancer for macrophage-selective expression [18,19]. A preferential and inducible expression of SAA1 in the lung tissue was observed. The SAA1 transgenic mice were characterized in peritonitis and acute lung injury models. Contrary to the widely claimed proinflammatory activities of SAA, transgenic mice expressing SAA1 did not develop spontaneous inflammation and instead showed reduced inflammatory cytokine expression, diminished neutrophil infiltration in the lungs, improved survival and significantly reduced endotoxin levels when challenged with LPS or cecal ligation and puncture (CLP). We found that SAA1 binds LPS to form a complex that promotes LPS clearance by macrophages. Administration of an SAA1-derived peptide that disrupts SAA1 binding to LPS reversed the protective effect and caused elevated endotoxin levels in the lungs and in serum, suggesting that acute-phase SAA is a host-derived anti-LPS protein.

## Results

### Transgenic expression of human SAA1 in mice

Elevated expression of acute-phase SAA may result from Gram-negative bacterial infection and exposure to LPS, but whether and how SAA regulates LPS-induced inflammatory response remains unknown. To evaluate the *in vivo* functions of acute-phase SAA in inflammation, we generated transgenic (Tg) mice expressing human SAA1 (hSAA1) using the enhancer and promoter from macrophage scavenger receptor A (SR-A) [18,19] (Fig 1A). A total of 98 founders and F1 progeny mice were analyzed, and three original founders were chosen for further characterization. Transgenic expression of human SAA1 was determined at the mRNA level in mouse macrophages (Fig 1B) and various mouse tissues (Fig 1C) using specific oligonucleotide primers. The human SAA1 transcript was most abundant in the lungs and testes based on the results of RT–PCR (Fig 1C). Using an antibody selectively detecting human SAA1, the transgene product was found at high abundance in the lungs and testes, and at lower levels in other mouse tissues based on Western blotting (Fig 1D). Bronchial lavage macrophages from the Tg but not the WT mice expressed the human SAA1 (inset, Fig 1D). Staining of lung tissue sections found colocalization of human SAA1 protein with the macrophage marker CD68 in the Tg mice (Fig 1E). Immunofluorescent staining of lung lavage macrophages confirmed the expression of human SAA1 (green) in CD68-positive cells (red, Fig 1F).

Human SAA1 was found at the basal level of 37 $\pm$ 4.12 ng per milligram of lung tissue proteins in the SAA1-Tg mice without challenge (Fig 1G). Consistent with the inducible nature of the SR-A promoter [18,19], LPS administration (*i.p.* and *i.t.*) and cecal ligation and puncture (CLP) further increased the expression levels of SAA1 in the lung tissue (Fig 1G) and in serum (Fig 1H). These findings demonstrated that the transgenic mice retained the feature of inducible SAA1 expression as seen in humans during acute-phase response. The SAA1-Tg mice were therefore used for further evaluation of the *in vivo* functions of acute-phase SAA.

### Transgenic SAA1 partially protects mice against CLP- and LPS-induced acute lung injury

CLP results in polymicrobial infection of the peritoneal cavity that can lead to sepsis, major organ failure, and death [20]. We compared the survival rates between WT and SAA1-Tg mice in a CLP sepsis model. Ninety-six hours after CLP, 86% of the WT mice were found dead, whereas 55% of the Tg mice survived ($P = 0.0137$ between groups) and all control mice with sham operation survived the procedure (Fig 2A). An examination of the lung histology found markedly reduced neutrophil infiltration and well-preserved alveolar structure in the SAA1-Tg mice compared to WT littermates 24 h after CLP (Fig 2B). Lung tissue expression of mouse IL-6 and TNFα, major inflammatory cytokines produced during systemic inflammation and acute lung injury, remained low in unchallenged SAA1-Tg mice (Fig 2C, Ctrl) despite published reports that SAA1 could induce the expression of these proinflammatory cytokines *in vitro* (reviewed in Ref. [10]). CLP increased the expression levels of both IL-6 and TNFα, but a significantly lower level of expression was seen in the Tg mice compared with the WT mice ($P < 0.01$). Of interest, the transcript of IL-10, an anti-inflammatory cytokine [21], was significantly higher in the lungs of the Tg mice than the WT littermates ($P < 0.01$). Similar changes in the expression of these cytokines were observed at the protein level in serum samples, although the difference in IL-10 expression was not statistically significant (Fig 2D, third bar graph). These observations suggest that transgenic expression of human SAA1 did not induce spontaneous inflammation in unchallenged mice, but suppressed the inflammatory response resulting from CLP-induced polymicrobial infection.

To further understand the mechanisms for SAA1-mediated suppression of lung inflammation, LPS-induced acute lung injury was performed on the SAA1-Tg mice and their WT littermates. Intraperitoneal administration of LPS (*i.p.*, 5 mg/kg) led to abundant neutrophil infiltration into the lungs of WT mice (Fig 3A, lower left panel), as quantified by an elevated lung myeloperoxidase (MPO) activity (Fig 3B). In comparison, the SAA1-Tg mice showed fewer neutrophils in lung tissue sections (Fig 3A, lower right panel) and significantly lower levels of the MPO activity (Fig 3B). At a higher dose, LPS (15 mg/kg) caused a significant elevation in lung vascular permeability, as evidenced by increased leakage of Evans blue albumin (EBA) into the lung tissue. In contrast, the Tg mice showed lower basal levels of lung EBA content, and there was no significant increase in EBA in the lung tissue after LPS stimulation (Fig 3C). Similar to what was seen in the CLP model, administration of LPS resulted in higher levels of TNFα and IL-6 expression in WT mice than in SAA1-Tg mice, whereas changes of IL-10 expression was in an opposite direction in the lungs (third bar graph in Fig 3D) and in serum (third bar graph in Fig 3E).

### Transgenic SAA1 offers no protection against TNFα-induced lung inflammation

To investigate whether transgenic expression of human SAA1 provides a general anti-inflammation mechanism, SAA1-Tg mice

 

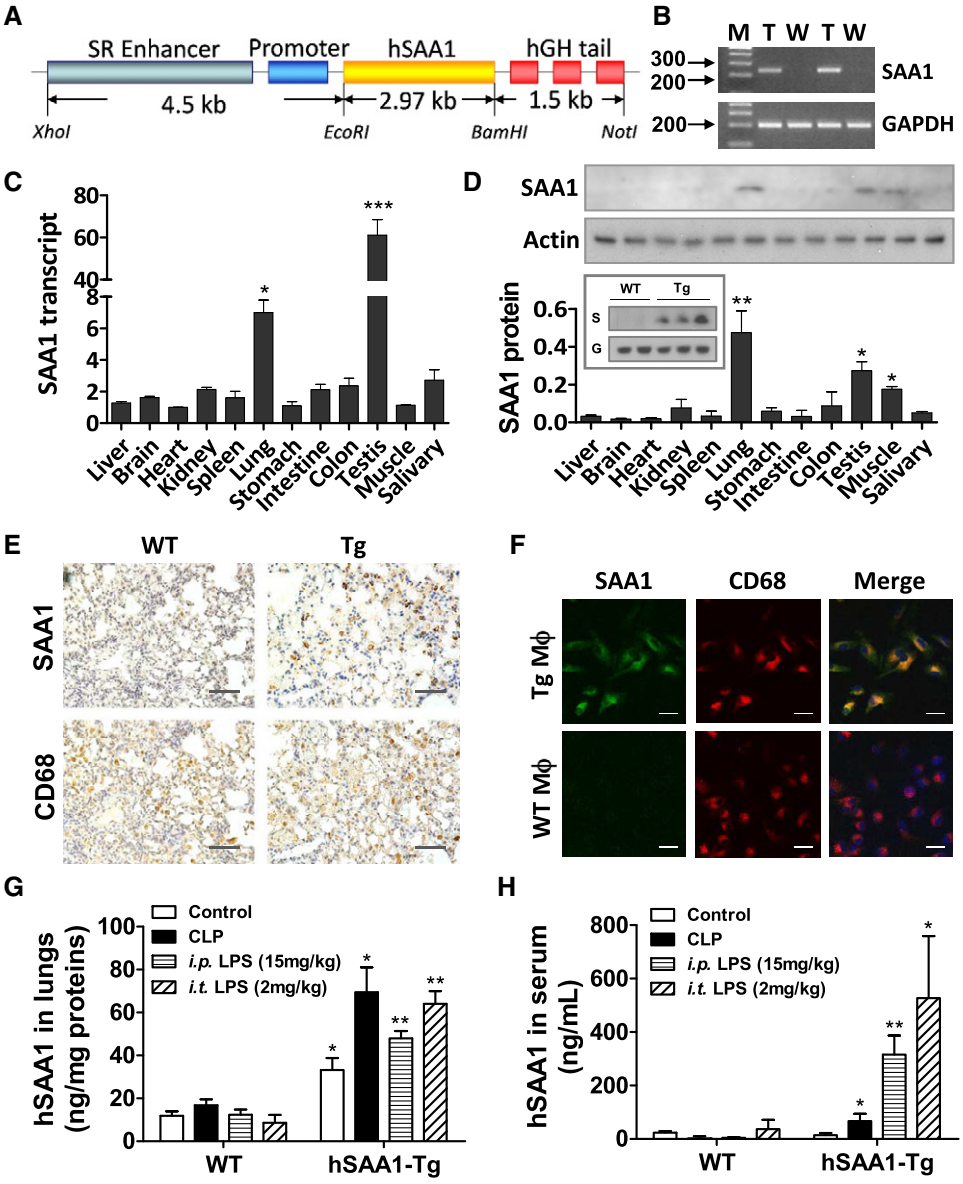


**Figure 1. Transgenic expression of human SAA1 in mice.**

A Schematic representation of the hSAA1 transgene (Tg) using the scavenger receptor A (SR-A) enhancer and promoter.

B RT–PCR analysis of human SAA1 transcripts in macrophages from WT (W) and SAA1-Tg (T) mice. M, molecular weight markers. GAPDH was used as a control.

C Comparison of SAA1 transcript in different tissues of the Tg mice ($n$ = 5) using qPCR. The SAA1 transcript level in the heart was set as 1 (baseline), against which the relative expression levels of SAA1 in other tissues were compared.

D Representative Western blots showing SAA1 protein expression in different tissues of the Tg mice. Five mice were examined, and the relative expression levels of SAA1 are shown in bar chart below, using the expression level in the heart as baseline for comparison. Inset: Western blot detection of human SAA1 (S) in alveolar lavage macrophages from WT ($n$ = 2) and Tg ($n$ = 3) mice. GAPDH (G) was used as a loading control.

E Immunohistochemistry staining of human SAA1 and CD68 in serial sections of lungs from WT and Tg mice. Three mice in each group were analyzed, and a representative set of images is shown. Scale bar, 200 μm.

F Immunofluorescence staining of SAA1 (green) and CD68 (red) in lung lavage macrophages from the Tg mice ($n$ = 5). A representative set of images is shown. Scale bar, 20 μm.

G, H Expression levels of human SAA1 in the lungs (G) and serum (H) of WT and SAA1-Tg mice (five in each group) without and with LPS stimulation (*i.p.* and *i.t.*). Data information: Data shown in (C, D, G, H) are means ± SEM based on triplicate measurements. *$P$ < 0.05, **$P$ < 0.01, and ***$P$ < 0.001 relative to baseline (C, D) or when compared with WT samples (G, H).

Source data are available online for this figure.

and their WT littermates were given intratracheal instillation of TNFα and the resulting lung inflammatory response was compared. Histological examination of mouse lung tissue sections identified damaged alveolar structure and increased neutrophil infiltration in both WT and Tg mice with no discernable difference (Fig 4A). Moreover, both Tg and WT mice showed similar

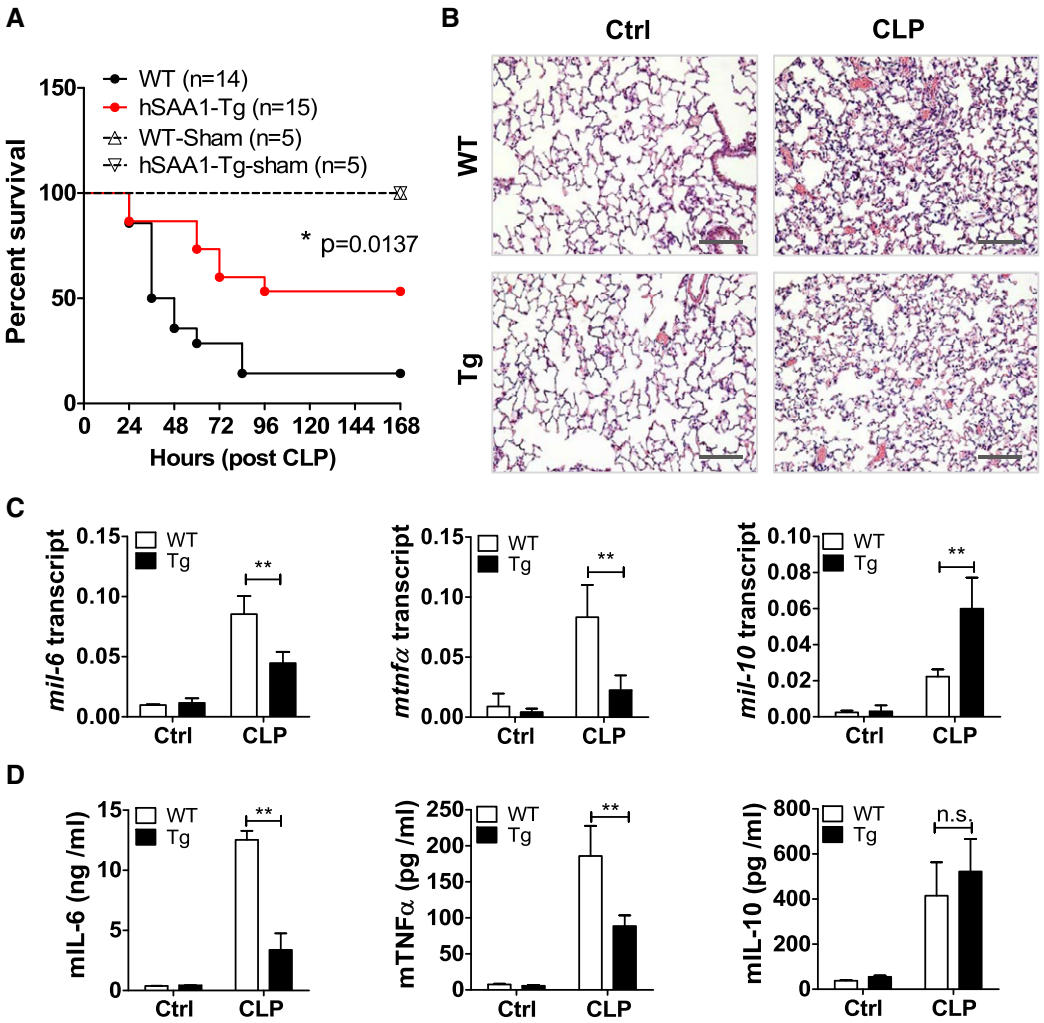


**Figure 2. SAA1 protects mice against CLP-induced lung inflammation and death.**

A Survival of the SAA1-Tg mice (closed red circles) was significantly better than their WT littermates (closed black circles) after CLP. All mice in sham groups (up-pointing open triangles for WT sham and down-pointing open triangles for Tg sham) survived. Sample size was predetermined with *a priori* power analysis and marked next to each sample group. Significance analysis was determined by log-rank (Mantel-Cox) test using the GraphPad Prism software.

B Representative images of H&E stained lung sections from WT and SAA1-Tg mice ($n$ = 5 each) 24 h after CLP, showing alveolar structures and leukocyte infiltration. Scale bar, 200 μm.

C Expression of selected cytokines at the mRNA level in mouse lung tissues 24 h after CLP ($n$ = 5 for each group).

D Expression of selected cytokine at the protein level in mouse serum measured by ELISA 24 h after CLP ($n$ = 4 for sham control group, $n$ = 8 for CLP group).

Data information: Data shown in (C, D) are means ± SEM based on triplicate measurements. **$P$ < 0.01 and n.s. not significant, using two-way ANOVA for multiple comparisons.

changes in MPO activity when challenged with TNFα (Fig 4B), and TNFα administration increased lung microvascular permeability in Tg mice and their WT littermates to a similar extent (Fig 4C). The lack of the protective effect was not due to insufficient induction of the transgenic human SAA1, as the serum level of hSAA1 rose significantly in the Tg mice following TNFα administration ($P$ < 0.01, Fig 4D). Despite a marked induction of human SAA1 expression, there was no significant increase in IL-6 and IL-1β expression levels in the serum of TNFα-treated mice (Fig 4E and F), suggesting that *i.t.* instillation of TNFα did not induce a systemic inflammatory response despite marked rise in SAA1 production. Taken together, these results indicate an absence of protection against TNFα-induced acute lung injury that was expected from transgenic expression of SAA1 should it produce a general anti-inflammatory effect.

### SAA1 binds LPS and reduces serum endotoxin level

The serum endotoxin levels in mice receiving CLP (Fig 5A) and intraperitoneal LPS administration were determined (Fig 5B). Both procedures caused a marked increase in serum endotoxin levels within 24 h, but the increase was significantly less in SAA1-Tg mice than in their WT littermates ($P$ < 0.01). Based on these findings, we postulated that overexpression of SAA1 might

 

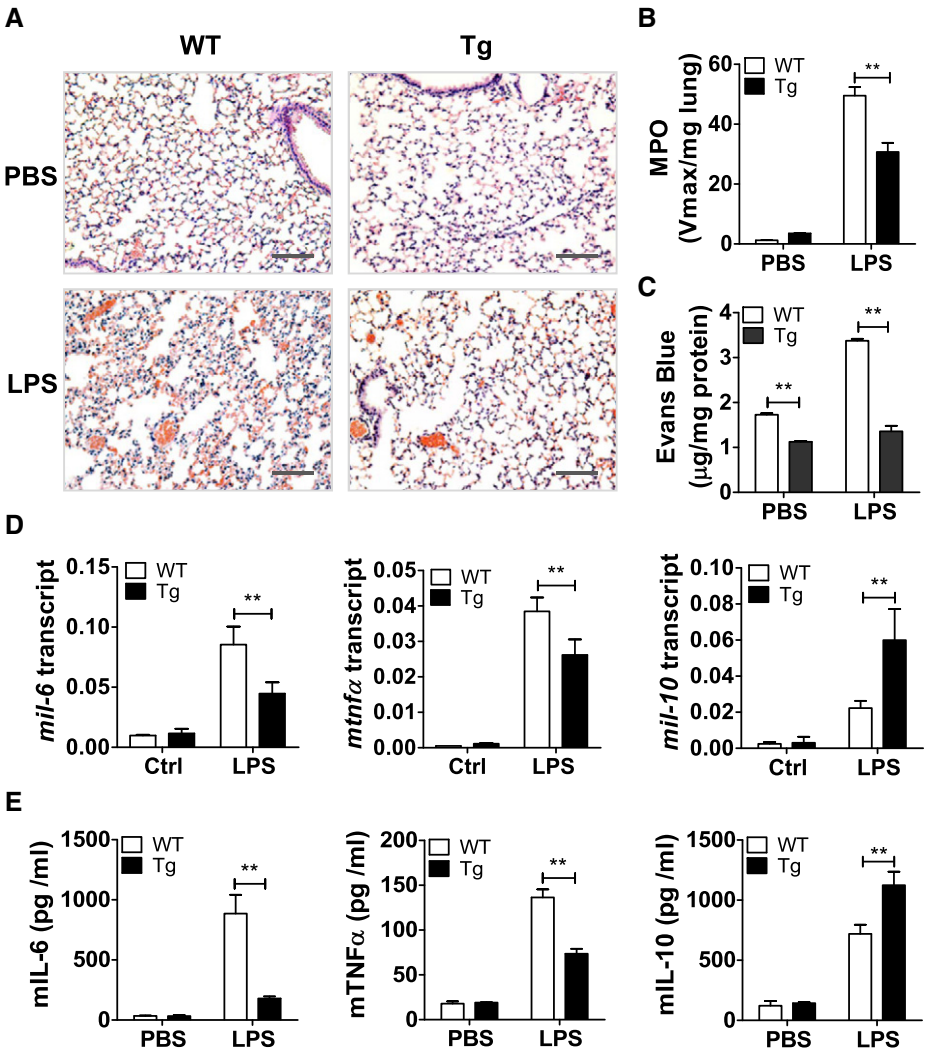


**Figure 3. Transgenic SAA1 protects mice against LPS-induced acute lung injury.**

A Representative images showing H&E stained sections from WT and SAA1-Tg mice ($n$ = 5 each type) 24 h after *i.p.* injection of LPS (5 mg/kg). Scale bar: 200 μm.

B Lung MPO activity in WT and SAA1-Tg mice 24 h after *i.p.* injection of LPS (5 mg/kg).

C Evans blue content in the lungs of WT and Tg mice 6 h after *i.p.* injection of LPS (15 mg/kg).

D Expression of selected cytokines at the mRNA level in mouse lungs 24 h after *i.p.* injection of LPS (5 mg/kg).

E Expression of selected cytokines at the protein level in mouse serum 24 h after *i.p.* injection of LPS.

Data information: Data shown in (B–E) are means ± SEM based on three experiments ($n$ = 6 mice/group). $^{**}P < 0.01$ between groups using two-way ANOVA for multiple comparisons.

alleviate acute lung injury by targeting LPS. To further explore this possibility, binding assays were conducted to determine an interaction between SAA1 and LPS. It was found that recombinant SAA1 purified from *E. coli* overexpression system or transfected human HEK293 cells could bind biotinylated LPS in a dose-dependent manner (Fig 5C and D). To confirm complex formation between SAA1 and LPS, native polyacrylamide gel electrophoresis and Western blotting were performed (Fig 5E). Biotin-LPS was detected by streptavidin-HRP (upper panel), while SAA1 was detected with an anti-SAA1 antibody (middle and lower panels). In addition to SAA1 monomers and oligomers, an SAA1 species that overlapped with the high molecular weight LPS species was detected by the anti-SAA1 antibody in the presence of LPS but not in its absence, suggesting formation of an SAA1-LPS complex. Using surface plasmon resonance (SPR) analysis, a direct interaction between SAA1 and LPS was confirmed (Fig 5F).

Using flow cytometry, we observed that SAA1 binding to LPS promoted macrophage uptake of FITC-LPS, as seen with an increased mean fluorescent intensity in the presence of SAA1 vs. its absence, after removal of cell surface-bound FITC-LPS (Fig 5G). SAA1 also facilitated the uptake of FITC-labeled LPS by CD68-positive cells (macrophages, red fluorescence) as observed using fluorescent confocal microscopy (Fig 5H).

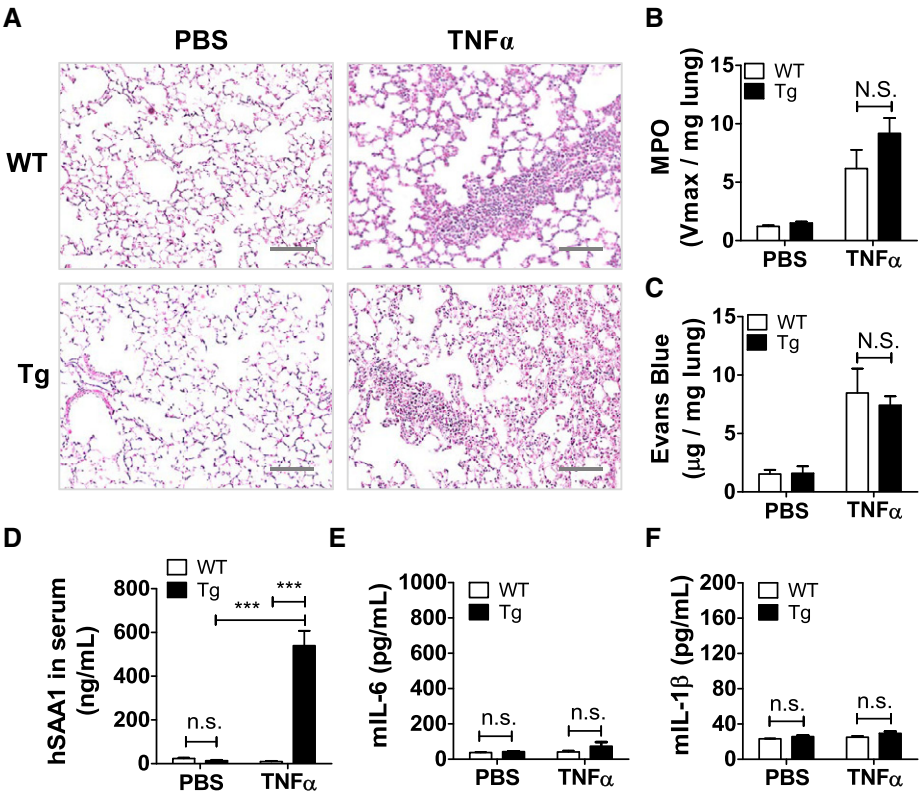


**Figure 4. Transgenic SAA1 does not protect against TNFα-induced lung injury.**

A Representative H&E stained lung sections from WT and SAA1-Tg mice ($n$ = 5 in each group examined) 6 h after intratracheal instillation of mouse TNFα (20 μg/kg, same below). Scale bar: 200 μm.

B Lung MPO activity in WT and SAA1-Tg mice 6 h after *i.t.* injection of mouse TNFα.

C Evans blue content in the lungs of WT and SAA1-Tg mice 6 h after *i.t.* injection of mouse TNFα.

D–F Serum levels of human SAA1 (D), mouse IL-6 (E), and IL-1β (F) determined 24 h after *i.t.* administration of TNFα as described above.

Data information: Data shown (B–F) are means ± SEM based on three measurements with five mice in each group; ***$P < 0.001$, *n.s.*, not statistically significant with two-way ANOVA for multiple comparisons.

### Blocking SAA1-LPS interaction exacerbates acute lung injury

The above findings suggest that SAA1 interacts directly with LPS and promotes LPS uptake, thereby contributing to the reduction in LPS concentration in the lung tissue and in serum. To further examine the biological functions of the SAA1-LPS interaction, a peptide-mediated competition approach was developed. Five peptides covering the entire lengths of mature SAA1 protein were prepared (Fig 6A). *In vitro* characterization of these peptides in SAA1-LPS-binding assays identified Pep 2 (a.a. 32–47) as being most potent in disrupting the interaction between SAA1 and LPS, in binding assays with a fixed concentration of the peptides and variable concentrations of LPS (Fig 6B) or a fixed concentration of LPS and variable concentrations of the peptides (Fig 6C). To examine its *in vivo* effect, Pep 2 or a control peptide with scrambled sequence was injected *i.v.* into SAA1-Tg mice immediately following CLP, and serum endotoxin levels were measured 24 h after the procedure. As shown in Fig 6D, SAA1-Tg mice receiving Pep 2 had significantly higher levels of endotoxin in serum than mice receiving the control peptide. There were also higher concentrations of serum IL-6 (Fig 6E) and TNFα (Fig 6F) in the Tg mice receiving Pep 2 compared to mice receiving the control peptide. Pep 2 had similar effects in WT mice under the same experimental conditions (Fig 6G–I). Mice receiving Pep 2 following CLP showed markedly increased MPO activity (Fig 6J) and increased production of IL-6 (Fig 6K) and TNFα (Fig 6L) in the lung tissue than mice receiving the control peptide. To determine whether Pep 2 could disrupt SAA1-LPS interaction *in vivo*, biotin-LPS was diluted with unconjugated LPS and *i.p.* administered. Either Pep 2 or the control peptide was then given *i.v.* to these mice. After 24 h, plasma SAA1 protein was captured by an immobilized anti-SAA1 antibody and the bound biotin-LPS was detected by streptavidin-HRP. As shown in Fig 6M, Pep 2 administration significantly reduced the amount of SAA1-bound biotin-LPS compared with the control peptide. Meanwhile, the plasma endotoxin level in mice receiving Pep 2 was higher than that in mice receiving the control peptide (Fig 6N). These findings demonstrate *in vivo* disruption of SAA1-LPS interaction by Pep 2, which led to changes in plasma endotoxin levels.

### Effect of transgenic SAA1 on phagocyte response to LPS

Experiments were conducted to identify potential mechanisms, in addition to promoting macrophage uptake of LPS, that might contribute to the protective effect of the transgenic SAA1. The ability of

 

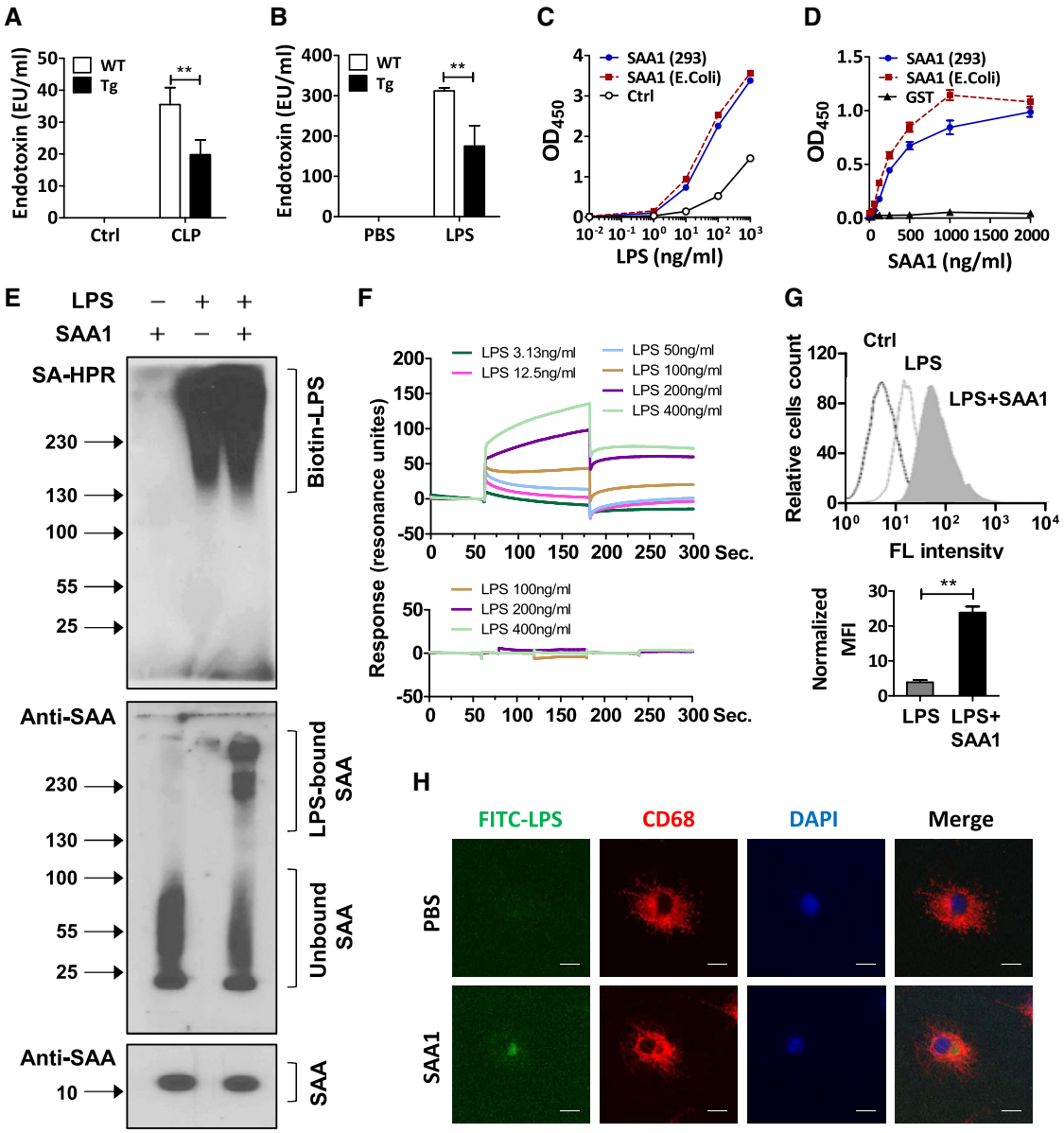


**Figure 5. SAA1 binding of LPS promotes LPS clearance.**

A, B Serum endotoxin levels were lower in SAA1-Tg mice than in WT littermates ($n$ = 5 in each group) 24 h after CLP (A) or *i.p.* injection of LPS (B, 5 mg/kg).

C, D Biotinylated LPS interacts with human SAA1 expressed in *Escherichia coli* (closed red squares) or in transfected HEK293T cells (closed blue circles) as a function of LPS concentrations (C) or SAA1 concentrations (D) ($n$ = 3). The SAA1 concentration used in (C) was 1 μg/ml. The LPS concentration used in (D) was 10 ng/ml.

E Complex formation between human SAA1 and LPS. Biotin-LPS was solubilized by sonication in PBS and incubated with human SAA1 for 2 h at room temperature. The mixture was loaded onto a 7.5% native polyacrylamide gel for electrophoresis. Western blots were prepared, and LPS was detected using streptavidin-HRP (upper panel). Human SAA1 was detected with an anti-SAA antibody (middle panel). As a control, SAA1 was also detected by Western blotting after SDS–PAGE to verify its integrity and equal loading.

F Surface plasmon resonance (SPR) analysis of SAA1-LPS interaction. Binding signals were detected by injecting various concentrations of LPS (3.13–400 ng/ml) over immobilized SAA1 that contains six histidines in its C-terminus and amine-coupled to the sensor chip. A representative sensorgrams showed the association and dissociation of LPS to/from SAA1. The lower panel shows control tracings recorded using GST instead of SAA1 for surface coating.

G Enhanced uptake of FITC-labeled LPS (LPS) by BMDMs in the absence or presence of human SAA1 (1 μM, 4 h). Cell surface FITC-LPS was then removed by proteinase K treatment for 30 min, and internalized FITC-LPS was determined by flow cytometry. Shown in upper panel is a representative histogram from five independent experiments. Shown in lower panel are normalized median fluorescence intensities (MFI, with background fluorescence subtracted) from the five experiments.

H Representative confocal fluorescent micrographs ($n$ = 3) showing FITC-LPS (green) internalization by BMDMs treated with PBS or SAA1 (1 μg/ml FITC-LPS, 1 μM SAA or PBS, 4 h). CD68 (red) and nuclei (blue) were also stained. Scale bar, 10 μm.

Data information: Data shown (A–D, G lower panel) are means ± SEM based on three measurements. $^{**}P < 0.01$ between different groups with two-way ANOVA for multiple comparison.
Source data are available online for this figure.

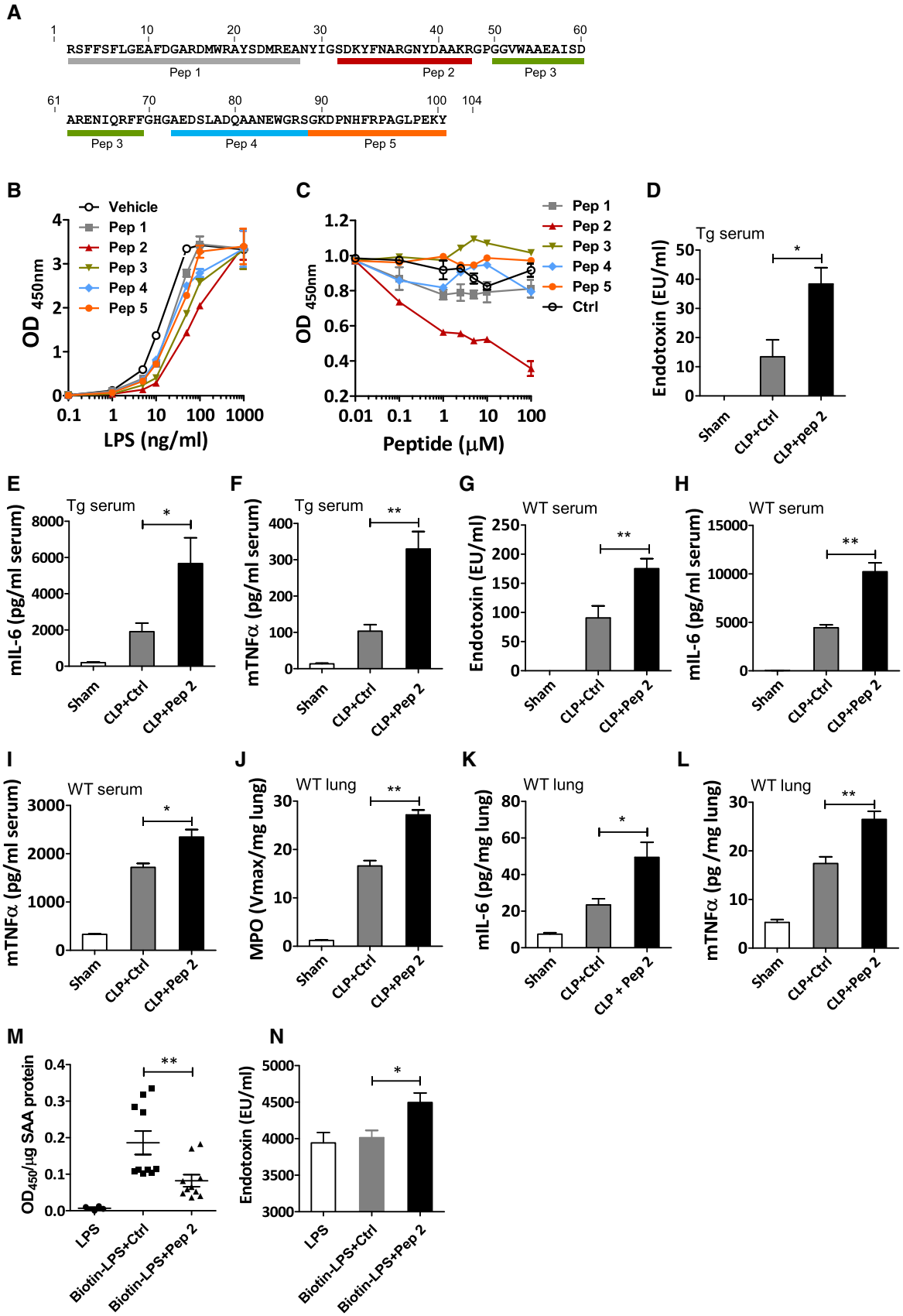


**Figure 6.**

**Figure 6. Blocking LPS interaction by Pep 2 partially reverses the protective action of SAA1.**

A Sequence of mature human SAA1 showing positions of the five peptides.

B, C Peptide blockade of biotin-LPS interaction with SAA1 as a function of different LPS concentrations (B, with each peptide used at 10 μM each), and by different concentrations of the peptide tested (C, with biotin-LPS used at 10 ng/ml). Human SAA1 was used at a concentration of 1 μg/ml. Data shown are means ± SEM based on three measurements.

D–F SAA1-Tg mice ($n$ = 5 in each group) that underwent CLP or sham operation were given *i.v.* Pep 2 or a peptide with scrambled sequence (N-KNADFDRKRYANRDYY-C) at 50 μg/mouse. After 24 h, serum levels of endotoxin (D), IL-6 (E) and TNFα (F) were measured.

G–I Same as in (D–F) but the procedures were carried out in WT mice ($n$ = 5 each group).

J–L Lungs were removed from WT mice that underwent CLP and received either Pep 2 or the control peptide, as described above for (D, E and F). Lung tissue MPO activity (G), lung tissue IL-6 (H), and TNFα (I) were determined as described in Materials and Methods.

M, N *In vivo* effect of disrupting LPS-SAA interaction by Pep 2. To test *in vivo* the effect of Pep 2 on SAA1-LPS interaction (M), biotin-LPS was diluted with unconjugated LPS (2:13) and injected *i.p.* into WT C57BL/6 mice ($n$ = 10) at a dose of 15 mg LPS/kg body weight. Either Pep 2 or the control peptide with scrambled sequence (50 μg/mouse) was given *i.v.* immediately following LPS administration. After 24 h, mouse plasma was collected and SAA protein was captured in a 96-well plate pre-coated with an anti-SAA1 antibody (clone 202D7, see Materials and Methods). After incubation for 2 h, unbound SAA1 and LPS were removed, and streptavidin-HRP was used for detection of the biotin-LPS bound to the captured SAA1. As a control, plasma was collected from mice receiving unconjugated LPS (15 mg/kg) without peptide injection. The amount of bound biotin-LPS was measured at $OD_{450}$ and normalized against the amount of captured SAA protein which was determined using ELISA. In (N), the endotoxin levels in the three testing groups described above were detected using an LAL kinetic kit as described in the Materials and Methods.

Data information: Data shown in (D–L) are means ± SEM based on three independent experiments and with five mice in each testing group. $*P < 0.05$ and $**P < 0.01$ between groups receiving Pep 2 and the control peptide, with one-way ANOVA for multiple comparisons. Data in (M, N) are shown as mean ± SEM. $**P < 0.01$, $*P < 0.05$, determined with unpaired two-tailed Student's $t$-test.

the LPS-SAA1 complex to induce macrophage activation was compared with that of LPS or SAA1 alone in BMDMs based on induced phosphorylation of ERK and p38 MAPK. As shown in Fig EV1, cells stimulated with LPS plus SAA1 responded with ERK and p38 MAPK phosphorylation to the same extent as cells receiving LPS and SAA1 alone. The results suggest that the LPS-SAA1 complex retained BMDM-activating capability, but did not produce an additive or synergistic effect that could result from the abilities of SAA1 to activate these cells through TLR4 and TLR2 [22,23]. To determine whether exposure to the transgenic SAA1 led to desensitization of TLR4, mouse BMDMs were preincubated with a sub-activation dose of SAA1 (10 nM) before stimulation with LPS (100 ng/ml). As shown in Fig EV2, preincubation with SAA1 potentiated the LPS-induced phosphorylation of ERK and p38 MAPK. Similar results were obtained from studies of bone marrow-derived neutrophils. In the latter cells, preincubation with SAA1 at a sub-activation dose (10 nM) did not desensitize subsequent response to WKYMVm (W-pep, a potent agonist for the formyl peptide receptors 1 and 2; [24]) based on the induced phosphorylation of ERK and p38 MAPK (Fig EV3). Finally, transgenic expression of human SAA1 in mice did not abrogate migration of neutrophils and lymphocytes to peritoneal cavity in response to WKYMVm or SAA1 (Fig EV4). These results indicate that low-level expression of transgenic SAA1 in unchallenged mice did not alter host phagocyte response to LPS or WKYMVm through desensitization.

## Discussion

Different models of SAA expression have been established to mimic SAA production during acute-phase response. Webb *et al* [25] conducted adenovirus vector-mediated expression of SAA1 in apoA-I-deficient mice. The adenoviral vector-mediated expression results in systemic elevation of SAA in the plasma and is therefore suitable for studies of SAA interaction with plasma components. Because acute-phase SAA is found in all inflammatory tissues, studies of SAA in these tissues have drawn increasing attention after reports of its immunomodulatory activities in the intestine [15,16]. The present study uses a transgenic approach to generate mice with inducible expression of acute-phase SAA1 in macrophages in order to study the regulatory functions of SAA1 in tissues where macrophages are abundant and contribute to local inflammation and immunity. In addition to the inducible feature, our approach allows for the production of lipid-free or lipid-poor SAA1 proteins that are crucial to studies of its interaction with cell surface receptors and pathogen-derived molecules such as LPS. The forms and sites of SAA production are important to experimental design, given that SAA in lipid-bound and lipid-free forms may produce different biological functions [26,27].

Using the SAA1 transgenic mice, we report for the first time that acute-phase SAA1 offers partial protection against LPS-induced inflammation and acute lung injury through direct binding to LPS and promotion of its clearance. Of interest, the protective effect was observed in mice undergoing CLP or receiving LPS administration, but not in mice receiving *i.t.* instillation of TNFα. Corroborating these observations, *in vitro* assays demonstrate binding of SAA1 with LPS and formation of a complex between SAA1 and LPS. The SAA1-Tg mice had lower plasma endotoxin level and higher survival rate than the WT mice following CLP, demonstrating a protective effect of the transgenic SAA1. Further supporting a protective role for SAA1, disruption of the SAA1-LPS interaction by a SAA1-derived peptide exacerbated lung inflammation and elevated serum endotoxin level following CLP. These observations show that inducible expression of acute-phase SAA1 may protect host against Gram-negative bacterial infection by reducing LPS-induced tissue injury.

A prominent feature of the SAA1-LPS interaction is the resulting complex that promotes LPS uptake by macrophages. Accelerated removal of LPS contributes to attenuated lung inflammatory cytokine expression, reduced neutrophil infiltration and microvascular leakage, and improved survival following CLP and systemic administration of LPS. Binding of SAA1 to LPS is shown using biotin-LPS and SAA1 produced in both *E. coli* and HEK 293 cells, suggesting that the source of the recombinant SAA1 is not critical to the interaction of SAA1 and LPS. In addition, surface plasmon resonance analysis has confirmed a direct interaction between SAA1 and LPS.

Finally, native polyacrylamide gel electrophoresis identifies an SAA1-LPS complex that migrates at reduced speed and overlaps with the expected position of LPS in the gel. Flow cytometry analysis and fluorescent confocal microscopy demonstrate enhanced uptake of FITC-LPS by macrophages in the presence of SAA1. The improved LPS uptake by tissue macrophages is consistent with reduced serum endotoxin levels in Tg mice receiving CLP. SAA1-LPS interaction is important for improved LPS clearance, as a SAA1-derived peptide has been shown to inhibit SAA1-LPS-binding *in vitro* and partially negates the endotoxin-lowering effect *in vivo*.

In addition to facilitating LPS removal through SAA1-LPS complex formation, there may be other mechanisms that contribute to the observed anti-inflammatory and tissue-protecting effects of the transgenic SAA1. Our study investigated the possibility that SAA1 binding neutralizes the proinflammatory activities of LPS. However, incubation of LPS with SAA1 under conditions that promote complex formation did not abrogate their ability to induce macrophage response such as agonist-induced phosphorylation of ERK and p38 MAPK. It is notable that although both LPS and SAA1 can activate TLR4 and SAA1 can additionally activate TLR2, no additive or synergistic effect was observed when both LPS and SAA1 were used together. These findings suggest that SAA1 may serve as an LPS antagonist or blocker. The possibility that sustained exposure to transgenic SAA1 leads to desensitization of TLR4 signaling was excluded since exposure of BMDMs to a low dose of SAA1 did not reduce LPS-stimulated phosphorylation of ERK and p38 MAPK, and preincubation with SAA1 potentiated LPS-induced ERK phosphorylation. Similar results were obtained in bone marrow-derived neutrophils, in which SAA1 preincubation did not attenuate subsequent response to WKYMVm, a potent agonist of the formyl peptide receptor 2 (FPR2) that is also a receptor of SAA1. Finally, increased IL-10 production in the lung tissue of CLP- and LPS-treated mice may contribute to the observed anti-inflammatory effect of SAA1; however, its role seems to be limited to the specific organ and tissues as the serum level of IL-10 was not significantly increased in the Tg mice.

Published studies have shown that SAA1 is proinflammatory and its expression is expected to exacerbate tissue inflammation and injury [10,28]. However, transgenic expression of SAA1 did not induce spontaneous inflammation, nor did it raise the basal level of endogenous proinflammatory cytokines in the present study. In contrast, the transgenic mice receiving CLP or LPS administration showed lower expression levels of TNFα, IL-6, and IL-1β than the WT mice. It is notable that the majority of studies showing the proinflammatory properties of SAA was conducted *in vitro* using a recombinant human SAA protein containing an added methionine at the N-terminus and two swapped amino acids from SAA2 at positions of 60 and 71. These substitutions may have altered the properties of the recombinant SAA protein [17,29,30]. Another study showed that SAA1 proteins purified from patients lacked the ability to induce proinflammatory cytokine expression but could induce G-CSF expression in mouse monocytic cells in a TLR2-dependent manner [26]. It is important to note that the biological activities of SAA1 are subject to regulation by factors present in specific tissue microenvironment. For example, binding to plasma HDL abrogates the cytokine-like activities of SAA proteins [26]. Moreover, increased secretion of proteases such as cathepsin B and cathepsin D in inflammatory tissues may accelerate proteolysis of mature SAA proteins [31], resulting in SAA fragments with properties that differ from those of full-length SAA [32,33]. These findings suggest that acute-phase SAA may play different roles in different tissue microenvironment.

The structural basis for SAA1 interaction with LPS has not been identified. Mature SAA1 is a 104-amino acid peptide with four alpha-helices [9]. The well-documented beta-pleated sheets in amyloid A were, however, entirely missing from the solved crystal structure. A recent study reports that, under low pH conditions (pH 3.5–4.5), SAA1 forms soluble oligomers that undergo an α-helix to β-sheet conversion catalyzed by lipid vesicles [27]. Pep 2 (a.a. 32–47) that disrupts SAA1-LPS interaction overlaps with the second helix of mature SAA1, suggesting that helix II or a 3D structure containing helix II is involved in LPS binding. In addition, the sequence of Pep 2 partially overlaps with SAA fragments (e.g., a.a. 11–58) that were found recently to suppress LPS-induced inflammatory response [33]. Based on available information, it is predicted that the amphipathic helical domains of SAA1 located in the N-terminal half of mature SAA1 are responsible for its lipophilic interaction including LPS binding. In addition, SAA has been reported to bind bacterial outer membrane protein A [34] and serves as an opsonin for bacterial clearance [35]. This property of SAA may contribute to the reduced inflammatory response in CLP-induced acute lung injury. In addition, SAA has been shown to potentiate neutrophil superoxide generation through activation of NADPH oxidase, thereby promoting killing of invading bacteria [36].

The present study may be physiologically relevant since LPS is one of the potent inducers of acute-phase SAA such as SAA1, and elevated SAA1 may bind LPS and promotes it clearance through a feedback mechanism. During acute-phase response, large amounts of SAA proteins are produced by hepatocytes and are subsequently released into blood circulation, where the newly synthesized SAA displaces ApoA-I and becomes a major apoprotein of HDL3 [37]. HDL is a major plasma protein that binds LPS and plays an important role in LPS removal [38,39]. In addition, expression of acute-phase SAA by tissue macrophages may promote LPS clearance, thereby reducing plasma endotoxin levels. Rapid LPS removal occurs in the liver through HDL interaction with receptors on liver sinusoidal endothelial cells, whereas macrophage uptake provides a sustained means for LPS removal from tissues infected with Gram-negative bacteria [39,40]. The scavenge receptor SR-BI [41,42], that is one of the SAA receptors, has been shown to mediate internalization of the SAA1-LPS complex [43]. Collectively, our findings suggest that tissue expression of SAA1 promotes clearance of LPS in infected tissues, thereby contributing to reduced endotoxin levels in the plasma. Future studies will be extended to sepsis patients in order to confirm a physiological role for acute-phase SAA in LPS clearance.

In conclusion, the present study has led to the identification of acute-phase SAA1 as an LPS-binding protein that limits the proinflammatory activities of LPS in mouse models of acute lung injury. Unlike HDL, a major LPS-binding protein with reduced concentration in septic plasma, SAA expression is markedly increased following bacterial infection and therefore can play an active role in LPS binding and removal. The present study is limited only to one of the inducible acute-phase SAA proteins. It is therefore

 

unclear whether other forms of SAA proteins, including SAA2 and SAA3, are also involved in LPS binding and clearance. Studies of different subtypes of SAA proteins have been conducted using mouse models of colitis and SAA gene knockout mice. These studies have shown that SAA1/2 and SAA3 display similar functions in host defense but the pattern of their induced expression is different. As a result, SAA1/2 and SAA3 play different but partially overlapping roles in the maintenance of antimicrobial activity and epithelial integrity, respectively [44,45]. Additional studies using SAA gene knockout mice will likely identify the different functions of these SAA subtypes in lung physiology. Despite these limitations, the findings of this study provide a clearer although no less complicated picture of SAA as an endogenous protein produced under various stress conditions that protects host against environmental insults. Future studies will focus on the mechanisms underlying the differences between *in vitro* assays of SAA1 and *in vivo* studies of the SAA1-Tg mice, including possible cleavage of SAA at sites of inflammation, the functional difference of SAA monomers and oligomers and the resulting preference for different SAA receptors. Understanding the protection mechanisms of acute-phase SAA may help to develop novel therapies for infectious and inflammatory diseases.

## Materials and Methods

### Animal studies

All procedures involving mice were carried out at the University of Illinois at Chicago and were approved by the Institutional Animal Care and Use Committee (IACUC) of the university. For all experiments with transgenic mice, WT littermate controls of both genders were used. A randomized approach of choosing mice was used throughout the study, using all mice with the correct genotype without bias.

### Reagents

Rabbit anti-human SAA antibody (H-84, sc-20651) was purchased from Santa Cruz Biotechnology. Rat anti-CD68 antibody (FA-11, ab53444) was obtained from Abcam. Mouse cytokines IL-6 and TNFα ELISA kits were obtained from Invitrogen (Carlsbad, CA, USA). Anti-mouse SAA1 monoclonal antibody (clone 202D7) was made in house against recombinant mouse SAA1 protein. Rabbit anti-Phospho-p44/42 MAPK (ERK1/2, Thr202/Tyr204) (197G2) monoclonal antibody, rabbit anti p44/42 MAPK (ERK1/2) antibody (9102S), rabbit anti-Phospho-p38 MAPK (Thr180/Tyr182) antibody (9211S), rabbit anti-p38 MAPK Antibody (9212S), and anti-GAPDH antibody (5174S) were purchased from Cell Signaling Technology (Danvers, MA, USA). LPS and FITC-labeled LPS from *E. coli O111: B4*, and 3,3′,5,5′-tetramethylbenzidine for myeloperoxidase activity determination assay were purchased from Sigma-Aldrich (St. Louis, MO, USA). Biotinylated LPS from *E. coli O111:B4* (LPS-EB Biotin) was obtained from InvivoGen (San Diego, CA, USA). Peptides used in the study were synthesized at the Protein Research Laboratory of the University of Illinois at Chicago, with purity of 95% or above tested by HPLC. Recombinant murine TNFα was purchased from PeproTech (Rocky Hills, NJ, USA).

### Generation of transgenic mice expressing human SAA1

The plasmid containing the human scavenger receptor A (SR-A) promoter/enhancer and other elements (pAL1) [18,19] necessary for chimeric transgene construction was a generous gift of Dr. Christopher Glass (University of California, San Diego). For macrophage-specific expression of SAA1, a 2.97-kb genomic DNA of human SAA1 gene was cloned into the *Eco*RI and *Bam*HI sites between the SR-A promoter and the human growth hormone splicing and polyadenylation sites (Fig 1A). Correct insertion of the chimeric transgene was confirmed by DNA sequencing. The SRA-hSAA1 transgene (8.97 kb) was isolated by digestion with *Xho*I and *Not*I, purified by agarose gel electrophoresis, and injected into fertilized mouse eggs obtained from superovulated female mice (FVB/N). The injected eggs were transferred to surrogate females. Offspring was screened for integration of the transgene by PCR amplification of genomic DNA with the upstream primer 5′-TT GCTGAGGCCTGCCAGGAACTAGG-3′ and the downstream primer 5′-AGTGATGCGTCTACCTGGCAAGAGCC-3′, with an expected 837 bp product. Southern blot analysis was further performed on genomic DNA to confirm transgene integration in the transgenic founder lines. Transgenic mice that had incorporated the transgene into the germ line were bred and backcrossed with C57BL/6 mice for over 10 generations. All experiments involving mice were conducted at the University of Illinois at Chicago using protocols approved by the Institutional Animal Care and Use Committee of the University, based on National Institutes of Health Guide for the Care and Use of Laboratory Animals.

### Measurement of human SAA1 expression

WT and SAA1-Tg mice were injected intraperitoneally with 2 ml of 3% thioglycollate solution, and macrophages were harvested 3 days later by lavage of the peritoneal cavity. The peritoneal macrophages were resuspended in RPMI 1640 with 10% fetal bovine serum and allowed for adhesion to cell culture dishes for 24 h. Total RNA from the adherent cells was extracted using RNeasy plus kit (Qiagen, Hilden, Germany). The protein and total RNA were extracted from different mouse tissues using RIPA buffer (Cell Signaling Technology) and TRIzol (Invitrogen). The tissue expression profile of human SAA1 was determined by real-time PCR with primers 5′-CTGCAGAAGTGATCAGCG-3′ and 5′-ATTGTGTACCCTCTCCCC-3′. Protein expression of the transgenic SAA1 in various mouse tissues was estimated by Western blotting with an antibody selective for human SAA.

### Cecal ligation and puncture (CLP) sepsis model

CLP sepsis was induced as described previously [20]. In brief, mice (12- to 16-week-old with equal number of each gender) were anesthetized by intraperitoneal administration of ketamine (100 mg/kg body weight; same below) and xylazine (8 mg/kg). The cecum was ligated at about 1 cm from the end and then subjected to a double "through and through" perforation with a 22-gauge needle. Sham-operated mouse underwent the same procedure except for ligation and puncture of the cecum. After the procedure, analgesia (Buprenorphine, 0.1 mg/kg, *s.c.*) was applied immediately and every 24 h thereafter for 3 days. At these time points, volume

support (prewarmed 0.9% NaCl, 0.05 ml/g body weight) was given through subcutaneous injection. The survival of mice was observed every 6 h and analyzed by log-rank test (using Prism software (ver. 5.0) by GraphPad, San Diego, CA, USA). For CLP-induced mouse lung injury, lung tissue was collected 24 h after sepsis and subject to immunohistochemistry and cytokine analyses.

#### Acute lung injury models

LPS- or TNFα-induced acute lung injury models were performed as previous description [46]. For LPS-induced acute lung injury, mice (three of each gender) were injected *i.p.* with LPS at 5–15 mg/kg body weight. For TNFα-induced acute lung injury, mouse TNFα (20 μg/kg) was given through intratracheal instillation. Twenty-four hours after *i.p.* injection of LPS and 6 h after *i.t.* instillation of TNFα, mouse lungs were perfused free of blood and instilled with 10% formalin through trachea at a pressure of 20–25 cm $H_2O$. Twenty-four hours after fixation, mouse lungs were embedded in paraffin. Lung sections (5 μm) were made for H&E stain.

Mouse lung microvascular permeability was determined as described previously [47]. Briefly, mice were *i.v.* injected with Evans blue albumin (EBA, Sigma, 20 mg/kg) through tail vein 30 min before the termination of a 6 h TNFα- or LPS-induced ALI to assess vascular leakage. After 30 min, the lungs were perfused with PBS and excised out of thoracic cavity. After homogenization in PBS (1 ml per 100 mg of lung tissue), lungs were further incubated with the addition of two volumes of formamide (Sigma) for 18 h at 60°C. At the end of this incubation, the homogenate was centrifuged at 93,000 *g* for 30 min and the supernatant was used to determine optical density spectrophotometrically at 620 nm. A standard curve was plotted, and EBA concentration in each sample was calculated as micrograms of Evans blue present in each milligram of lung tissue.

Cytokine expression in mouse lung and serum was measured 24 h after ALI. Transcripts of selected cytokines in mouse lung tissue were detected by real-time PCR using SYBR Green (Roche). The cytokine level in mouse serum was detected using ELISA.

#### Myeloperoxidase (MPO) activity assay

Infiltrating neutrophils in the lungs were detected based on MPO activity as described previously [48]. Mouse lungs were homogenized in 1.0 ml of 50 mM PBS (pH 6.0). After centrifugation at 13,000 × *g* for 30 min, the pellet was resuspended in 1 ml of 0.5% hexadecyltrimethylammonium bromide and treated with two cycles of freeze, thaw, and sonication. After centrifugation at 13,000 × *g* for 20 min at 4°C, the supernatant was incubated with 16 mM of 3,3′,5,5′-tetramethylbenzidine and 15 mM of $H_2O_2$, and absorbance at 655 nm was measured for 3 min. MPO activity based on lung tissue protein concentrations was calculated as the changes in absorbance over time.

#### Measurement of serum endotoxin

Mouse serum was collected 24 h after induction of sepsis by CLP or after *i.p.* injection of LPS. Endotoxin content in serum was detected using a kinetic *Limulus* amebocyte lysate (LAL) chromogenic endotoxin quantitation kit (Endochrome-K™ kit, Charles River, Wilmington, MA, USA) with slight modification of published methods [49]. In brief, 50 μl of mouse serum was diluted 1:10 with LAL reagent water (LRW) provided in the kit and heat-inactivated at 70°C for 15 min. The heat-inactivated samples were serially diluted 1:2, and aliquots (100 μl) of samples were transferred to a sterile 96-well plate. LAL (0.1 ml, ambient temperature) was quickly added to each well. For detection, standards supplied in the kit with the range from 0.005 to 50 EU/ml, the positive control, negative control, and blood collection tube control were performed at the same time with serum samples. Endotoxin concentrations were determined by measuring kinetic absorbance at 405 nm at 37°C following the instructions of the manufacturer, in a SpectraMAX 340 plate reader (Molecular Devices, San Jose, CA, USA) and plotted as EU per milliliter of serum.

#### LPS-binding assay

Binding of LPS to SAA1 was detected using biotinylated LPS (biotin-LPS, InvivoGen). Rabbit anti-SAA antibody (clone H-84, Santa Cruz Biotechnology) was used for pre-coating a 96-well EIA plate (Sigma-Aldrich) at 10 μg/ml in PBS at 4°C. After washing with PBST (0.1% Tween-20 in PBS) for three times, the plate was incubated with SAA1 at indicated concentrations for 2 h at 37°C. After washing with PBST three more times, various concentrations of biotin-LPS from 0 to 1 μg/ml was added to the wells and incubated at 37°C for 1 h. Streptavidin-HRP (Invitrogen) was used to detect biotin-LPS bond to the immobilized hSAA1 after incubation at 37°C for 30 min. After washing five times with PBST, the binding of LPS to SAA was colorized with the addition of the HRP substrate TMB stabilized chromagen (Invitrogen) and detected at an OD of 450 nm. For SAA1 peptide competition assay, 10 μM of each peptide was preincubated with 0–1,000 ng/ml of biotin-LPS, or 0–100 μM of each peptide was preincubated with 10 ng/ml of biotin-LPS at 37°C. After 30 min, the samples containing the SAA1 peptide and biotin-LPS were loaded onto a SAA1 immobilized EIA plate. Changes in absorbance at OD 450 nm were taken for samples with and without the competing peptides and were analyzed against binding of full-length SAA1.

#### SAA1-LPS complex formation

Complex formation between human SAA1 and LPS was determined using native PAGE and Western blotting analysis. Biotin-LPS (100 ng/ml, InvivoGen) was solubilized by sonication in PBS and incubated with SAA1 (500 ng/ml) for 2 h at room temperature. The SAA and LPS mixture was loaded onto a 7.5% native gel, and electrophoresis was performed in running buffer containing 25 mM Tris and 190 mM glycine. Western blots were prepared, and biotin-LPS was detected using streptavidin-HRP. Human SAA1 was detected with an anti-human SAA antibody (clone H-84, Santa Cruz Biotechnologies). As a control, the SAA1/LPS mixture was also analyzed by SDS–PAGE to confirm integrity of the protein and equal loading.

#### LPS uptake and internalization assays

For measurement of LPS uptake, mouse bone marrow-derived macrophages (BMDM, 1 × $10^5$ cells/ml) were incubated with 1 μg/ml of FITC-labeled LPS in RPMI 1640 for 4 h at 37°C. After incubation, BMDM cells were washed twice with PBS and further treated with 250 μg/ml proteinase K (Sigma-Aldrich) in HBSS for 30 min at room temperature to remove cell surface protein-bound LPS [50].

 

The remaining LPS was taken as intracellular and measured by flow cytometry. To evaluate the participation of SAA1 in LPS uptake, BMDM cells were incubated with human SAA1 (1 μM) and FITC-LPS (1 μg/ml) for 4 h before measurement of FITC-LPS uptake as described above.

For FITC-LPS internalization, BMDM cells were incubated with 1 μg/ml FITC-LPS with or without 1 μM SAA1 for 4 h at 37°C. Thereafter, the cells were fixed and permeabilized using 0.1% Triton X-100. CD68 was visualized using a rat anti-CD68 antibody (Abcam) and a fluorescently labeled anti-rat IgG as secondary antibody (Invitrogen). Nuclei were counterstained with ProLong Gold (Invitrogen). Images were acquired on a Zeiss LSM 880 confocal microscope.

#### Surface plasmon resonance (SPR) analysis

SPR experiments were conducted on a Biacore T200 instrument (GE Healthcare) by standard amine coupling. Full-length human SAA1 with C-terminal 6 × His was expressed in *E. coli* (BL21 DE3) and amine-coupled to a Biacore CM5 sensor chip (3,900 RUs). LPS (from *E. coli* O111:B4) was diluted to 100 μg/ml in the HBS-P running buffer (0.01 M HEPES, pH 7.4, 0.15 M NaCl, 0.005% surfactant P20) and run sequentially over the immobilized SAA1. The analytes were injected for 3 min at a flow rate of 25 μl/min and then allowed to dissociate for 10 min in the running buffer. As a control, GST instead of SAA1 was used for surface coating.

#### Statistical analysis

Data were expressed as means ± SEM. Differences between groups of samples were evaluated with Student's *t*-test, one-way ANOVA, or two-way ANOVA with Prism software (GraphPad). A *P*-value $\leq 0.05$ was considered statistically significant.

## Data availability

The authors declare that the data supporting the findings of this study are available within the paper and from the corresponding author upon reasonable request.

**Expanded View** for this article is available online.

### Acknowledgements
We thank Prof. Christopher Glass (University of California, San Diego) for providing the SR-A promoter/enhance plasmid. We also thank Mr. Jun Tian and Dr. Roberta Franks (Transgenic Production Service, University of Illinois at Chicago) for their assistance in generating the SAA1 transgenic mice and Dr. Hyun Lee (College of Pharmacy, University of Illinois at Chicago) for assistance in surface plasmon resonance analysis. This work was supported in part by R56 AI040176 from the National Institutes of Health. R.D.Y. received grant support from the Fundo para o Desenvolvimento das Ciências e da Tecnologia (026/2016/A1 and 072/2015/A1) and the University of Macau (MYRG2016-00152-ICMS-QRCM and CPG2015-00018-ICMS).

### Author contributions
NC designed the project, performed the experiments, analyzed data, and wrote the manuscript. YL designed and performed part of the *in vivo* experiments. XD provided critical support to the revision. RDY designed the project and wrote the manuscript.

### Conflict of interest
The authors declare that they have no conflict of interest.

## References

1. Ferrandon D, Imler JL, Hoffmann JA (2004) Sensing infection in *Drosophila*: toll and beyond. *Semin Immunol* 16: 43 – 53
2. Kushner I, Rzewnicki D (1999) Acute phase response. In *Inflammation: basic principles and clinical correlates*, Gallin JI, Snyderman R (eds), pp 317 – 329. Philadelphia, PA: Lippincott Willams & Wilkins
3. Gabay C, Kushner I (1999) Acute-phase proteins and other systemic responses to inflammation. *N Engl J Med* 340: 448 – 454
4. Uhlar CM, Whitehead AS (1999) Serum amyloid A, the major vertebrate acute-phase reactant. *Eur J Biochem* 265: 501 – 523
5. Malle E, Sodin-Semrl S, Kovacevic A (2009) Serum amyloid A: an acute-phase protein involved in tumour pathogenesis. *Cell Mol Life Sci* 66: 9 – 26
6. Kisilevsky R (1991) Serum amyloid A (SAA), a protein without a function: some suggestions with reference to cholesterol metabolism. *Med Hypotheses* 35: 337 – 341
7. Kisilevsky R, Manley PN (2012) Acute-phase serum amyloid A: perspectives on its physiological and pathological roles. *Amyloid* 19: 5 – 14
8. Uhlar CM, Burgess CJ, Sharp PM, Whitehead AS (1994) Evolution of the serum amyloid A (SAA) protein superfamily. *Genomics* 19: 228 – 235
9. Lu J, Yu Y, Zhu I, Cheng Y, Sun PD (2014) Structural mechanism of serum amyloid A-mediated inflammatory amyloidosis. *Proc Natl Acad Sci USA* 111: 5189 – 5194
10. Ye RD, Sun L (2015) Emerging functions of serum amyloid A in inflammation. *J Leukoc Biol* 98: 923 – 929
11. de Beer MC, Webb NR, Wroblewski JM, Noffsinger VP, Rateri DL, Ji A, van der Westhuyzen DR, de Beer FC (2010) Impact of serum amyloid A on high density lipoprotein composition and levels. *J Lipid Res* 51: 3117 – 3125
12. Sun L, Ye RD (2016) Serum amyloid A1: structure, function and gene polymorphism. *Gene* 583: 48 – 57
13. Badolato R, Wang JM, Murphy WJ, Lloyd AR, Michiel DF, Bausserman LL, Kelvin DJ, Oppenheim JJ (1994) Serum amyloid A is a chemoattractant: induction of migration, adhesion, and tissue infiltration of monocytes and polymorphonuclear leukocytes. *J Exp Med* 180: 203 – 209
14. Patel H, Fellowes R, Coade S, Woo P (1998) Human serum amyloid A has cytokine-like properties. *Scand J Immunol* 48: 410 – 418
15. Sano T, Huang W, Hall JA, Yang Y, Chen A, Gavzy SJ, Lee JY, Ziel JW, Miraldi ER, Domingos AI *et al* (2015) An IL-23R/IL-22 circuit regulates epithelial serum amyloid A to promote local effector Th17 responses. *Cell* 163: 381 – 393
16. Atarashi K, Tanoue T, Ando M, Kamada N, Nagano Y, Narushima S, Suda W, Imaoka A, Setoyama H, Nagamori T *et al* (2015) Th17 cell induction by adhesion of microbes to intestinal epithelial cells. *Cell* 163: 367 – 380
17. Bjorkman L, Raynes JG, Shah C, Karlsson A, Dahlgren C, Bylund J (2010) The proinflammatory activity of recombinant serum amyloid A is not shared by the endogenous protein in the circulation. *Arthritis Rheum* 62: 1660 – 1665
18. Horvai A, Palinski W, Wu H, Moulton KS, Kalla K, Glass CK (1995) Scavenger receptor A gene regulatory elements target gene expression

 

to macrophages and to foam cells of atherosclerotic lesions. *Proc Natl Acad Sci USA* 92: 5391 – 5395

19. Lemaitre V, O'Byrne TK, Dalal SS, Tall AR, D'Armiento JM (1999) Macrophage-specific expression of human collagenase (MMP-1) in transgenic mice. *Ann N Y Acad Sci* 878: 736 – 739
20. Rittirsch D, Huber-Lang MS, Flierl MA, Ward PA (2009) Immunodesign of experimental sepsis by cecal ligation and puncture. *Nat Protoc* 4: 31 – 36
21. Moore KW, de Waal Malefyt R, Coffman RL, O'Garra A (2001) Interleukin-10 and the interleukin-10 receptor. *Annu Rev Immunol* 19: 683 – 765
22. Cheng N, He R, Tian J, Ye PP, Ye RD (2008) Cutting edge: TLR2 is a functional receptor for acute-phase serum amyloid A. *J Immunol* 181: 22 – 26
23. Sandri S, Rodriguez D, Gomes E, Monteiro HP, Russo M, Campa A (2008) Is serum amyloid A an endogenous TLR4 agonist? *J Leukoc Biol* 83: 1174 – 1180
24. Le Y, Gong W, Li B, Dunlop NM, Shen W, Su SB, Ye RD, Wang JM (1999) Utilization of two-seven-transmembrane, G protein-coupled receptors, formyl peptide receptor-like 1 and formyl peptide receptor, by the synthetic hexapeptide WKYMVm for human phagocyte activation. *J Immunol* 163: 6777 – 6784
25. Webb NR, de Beer MC, van der Westhuyzen DR, Kindy MS, Banka CL, Tsukamoto K, Rader DL, de Beer FC (1997) Adenoviral vector-mediated overexpression of serum amyloid A in apoA-I-deficient mice. *J Lipid Res* 38: 1583 – 1590
26. Kim MH, de Beer MC, Wroblewski JM, Webb NR, de Beer FC (2013) SAA does not induce cytokine production in physiological conditions. *Cytokine* 61: 506 – 512
27. Jayaraman S, Gantz DL, Haupt C, Gursky O (2017) Serum amyloid A forms stable oligomers that disrupt vesicles at lysosomal pH and contribute to the pathogenesis of reactive amyloidosis. *Proc Natl Acad Sci USA* 114: E6507 – E6515
28. Eklund KK, Niemi K, Kovanen PT (2012) Immune functions of serum amyloid A. *Crit Rev Immunol* 32: 335 – 348
29. Christenson K, Bjorkman L, Ahlin S, Olsson M, Sjoholm K, Karlsson A, Bylund J (2013) Endogenous acute phase serum amyloid A lacks pro-inflammatory activity, contrasting the two recombinant variants that activate human neutrophils through different receptors. *Front Immunol* 4: 92
30. van den Brand B, Waterborg C, van den Berg W, van de Loo F (2013) Is the serum amyloid A we use really serum amyloid A? Comment on the article by Connolly et al.. *Arthritis Rheum* 65: 283 – 290
31. Rocken C, Menard R, Buhling F, Vockler S, Raynes J, Stix B, Kruger S, Roessner A, Kahne T (2005) Proteolysis of serum amyloid A and AA amyloid proteins by cysteine proteases: cathepsin B generates AA amyloid proteins and cathepsin L may prevent their formation. *Ann Rheum Dis* 64: 808 – 815
32. De Buck M, Gouwy M, Berghmans N, Opdenakker G, Proost P, Struyf S, Van Damme J (2018) COOH-terminal SAA1 peptides fail to induce chemokines but synergize with CXCL8 and CCL3 to recruit leukocytes via FPR2. *Blood* 131: 439 – 449
33. Zhou H, Chen M, Zhang G, Ye RD (2017) Suppression of lipopolysaccharide-induced inflammatory response by fragments from serum amyloid A. *J Immunol* 199: 1105 – 1112
34. Hari-Dass R, Shah C, Meyer DJ, Raynes JG (2005) Serum amyloid A protein binds to outer membrane protein A of gram-negative bacteria. *J Biol Chem* 280: 18562 – 18567
35. Shah C, Hari-Dass R, Raynes JG (2006) Serum amyloid A is an innate immune opsonin for Gram-negative bacteria. *Blood* 108: 1751 – 1757
36. Bjorkman L, Karlsson J, Karlsson A, Rabiet MJ, Boulay F, Fu H, Bylund J, Dahlgren C (2008) Serum amyloid A mediates human neutrophil production of reactive oxygen species through a receptor independent of formyl peptide receptor like-1. *J Leukoc Biol* 83: 245 – 253
37. Hu W, Abe-Dohmae S, Tsujita M, Iwamoto N, Ogikubo O, Otsuka T, Kumon Y, Yokoyama S (2008) Biogenesis of HDL by SAA is dependent on ABCA1 in the liver *in vivo*. *J Lipid Res* 49: 386 – 393
38. Ulevitch RJ, Johnston AR, Weinstein DB (1981) New function for high density lipoproteins. Isolation and characterization of a bacterial lipopolysaccharide-high density lipoprotein complex formed in rabbit plasma. *J Clin Invest* 67: 827 – 837
39. Munford RS (2005) Detoxifying endotoxin: time, place and person. *J Endotoxin Res* 11: 69 – 84
40. Yao Z, Mates JM, Cheplowitz AM, Hammer LP, Maiseyeu A, Phillips GS, Wewers MD, Rajaram MV, Robinson JM, Anderson CL *et al* (2016) Blood-borne lipopolysaccharide is rapidly eliminated by liver sinusoidal endothelial cells via high-density lipoprotein. *J Immunol* 197: 2390 – 2399
41. Baranova IN, Vishnyakova TG, Bocharov AV, Kurlander R, Chen Z, Kimelman ML, Remaley AT, Csako G, Thomas F, Eggerman TL *et al* (2005) Serum amyloid A binding to CLA-1 (CD36 and LIMPII analogous-1) mediates serum amyloid A protein-induced activation of ERK1/2 and p38 mitogen-activated protein kinases. *J Biol Chem* 280: 8031 – 8040
42. Cai L, de Beer MC, de Beer FC, van der Westhuyzen DR (2005) Serum amyloid A is a ligand for scavenger receptor class B type I and inhibits high density lipoprotein binding and selective lipid uptake. *J Biol Chem* 280: 2954 – 2961
43. Vishnyakova TG, Bocharov AV, Baranova IN, Chen Z, Remaley AT, Csako G, Eggerman TL, Patterson AP (2003) Binding and internalization of lipopolysaccharide by Cla-1, a human orthologue of rodent scavenger receptor B1. *J Biol Chem* 278: 22771 – 22780
44. Eckhardt ER, Witta J, Zhong J, Arsenescu R, Arsenescu V, Wang Y, Ghoshal S, de Beer MC, de Beer FC, de Villiers WJ (2010) Intestinal epithelial serum amyloid A modulates bacterial growth *in vitro* and pro-inflammatory responses in mouse experimental colitis. *BMC Gastroenterol* 10: 133
45. Zhang G, Liu J, Wu L, Fan Y, Sun L, Qian F, Chen D, Ye RD (2018) Elevated expression of serum amyloid A 3 protects colon epithelium against acute injury through TLR2-dependent induction of neutrophil IL-22 expression in a mouse model of colitis. *Front Immunol* 9: 1503
46. Qian F, Deng J, Gantner BN, Flavell RA, Dong C, Christman JW, Ye RD (2012) Map kinase phosphatase 5 protects against sepsis-induced acute lung injury. *Am J Physiol Lung Cell Mol Physiol* 302: L866 – L874
47. Naikawadi RP, Cheng N, Vogel SM, Qian F, Wu D, Malik AB, Ye RD (2012) A critical role for phosphatidylinositol (3,4,5)-trisphosphate-dependent Rac exchanger 1 in endothelial junction disruption and vascular hyperpermeability. *Circ Res* 111: 1517 – 1527
48. Qian F, Deng J, Cheng N, Welch EJ, Zhang Y, Malik AB, Flavell RA, Dong C, Ye RD (2009) A non-redundant role for MKP5 in limiting ROS production and preventing LPS-induced vascular injury. *EMBO J* 28: 2896 – 2907
49. Fukui H, Brauner B, Bode JC, Bode C (1991) Plasma endotoxin concentrations in patients with alcoholic and non-alcoholic liver disease: reevaluation with an improved chromogenic assay. *J Hepatol* 12: 162 – 169
50. Kitchens RL, Munford RS (1998) CD14-dependent internalization of bacterial lipopolysaccharide (LPS) is strongly influenced by LPS aggregation but not by cellular responses to LPS. *J Immunol* 160: 1920 – 1928

 